

INTERNATIONAL SOCIETY FOR SOIL MECHANICS AND GEOTECHNICAL ENGINEERING



This paper was downloaded from the Online Library of the International Society for Soil Mechanics and Geotechnical Engineering (ISSMGE). The library is available here:

<https://www.issmge.org/publications/online-library>

This is an open-access database that archives thousands of papers published under the Auspices of the ISSMGE and maintained by the Innovation and Development Committee of ISSMGE.

A Study on Stability of Clay Slopes by Centrifuge

Etude sur la Stabilité des Talus d'Argile par Centrifuge

M. MIKASA Dr., Professor,
 A. MOCHIZUKI Research Associate, Department of Civil Engineering, Osaka City University,
 Y. SUMINO Osaka Municipal Transportation Bureau, Japan

SYNOPSIS Two stability tests of clay slope models were carried out on centrifuge to investigate the mechanism of deformation and failure of slope quantitatively. The deformation of the slopes was observed by two kinds of markers. The slope of uniform strength (Test A) and of non-uniform strength increasing with depth (Test B) showed base failure and toe failure respectively. Safety factors of the slopes were estimated using the results of small cone tests in centrifugal acceleration field. And newly defined mobilization factor and deformation factor were applied to the test results to explain the mechanism of progressive failure.

1. INTRODUCTION

Centrifugal model test is now approved widely as the most effective means to investigate the behavior of soil structures such as slopes, foundations, etc. under the actual big self-weight in laboratory. The problem of slope stability, especially, has been investigated intensively by using centrifuge in USSR, United Kingdom and Japan. In our laboratory several series of slope stability test have been conducted for these 11 years both for the practical design works and for the basic research works.

This report is the latest of the latter, the purpose of which is to investigate the mechanism in which the deformation of clay slopes grows up into the failure quantitatively, especially from the viewpoint of progressive failure, and to check the reliability of the available analytical method for slope stability. For these purposes several improvements in the observation system have been tried and satisfactory results were obtained. In the analysis of the test results newly defined "mobilization factor m " and "deformation factor d " were used and clarified some aspects of the progressive failure of the model slopes.

2. CENTRIFUGE

The centrifuge used in this investigation (Fig.1) is almost the same in its mechanism but is enlarged in its dimensions and improved in the method of observation from the one which was introduced in our previous papers (Mikasa, Mochizuki, 1975, etc.). Its rotational radius was lengthened to 1.55m and the container was enlarged to 50x30x16.5cm³. A detachable framed side glass 12mm thick was used for convenience of model preparation. An induction motor of 11kw drives the machine and gives the model any arbitral acceleration under 200g. (g: gravitational acceleration)

3. MODEL PREPARATION AND TEST METHOD

3.1 Test Material

The material used here is high plastic alluvial clay sampled from Osaka Bay and sieved out under 0.6mm meshes. It was remolded at water content 170%, and put in a container (55x47x21cm³) at the height of 42cm and was consolidated for about 40days under 6t/m². The final water content was 75-80% and it had tendency

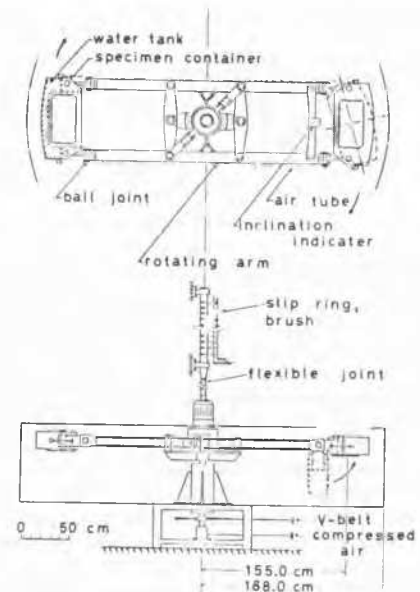


Fig. 1 Centrifugal apparatus

to be higher at the bottom of the container. A small cone test, however, showed almost uniform strength of $3.4 \pm 0.08 \text{t/m}^2$ expressed in q_u value except both ends of the soil block, which were trimmed off to assure homogeneity of specimen. The properties of the material are shown in Table I. This material exhibits the typical characteristics of alluvial clay in Japan, though sensitivity ratio is somewhat less than the usual undisturbed clay.

Table I Properties of material

Physical properties	Condition of material	Mechanical properties
G_s 2.657	γ_t 1.557t/m ³	q_u 3.41t/m ²
L.L 116.5%	w 77.8%	e_f 5.7%
P.L 38.1%	e 2.033	St 4.0
(Clay 56%	S_r 101.7%	P_y 5.2t/m ²
(Silt 41%		Cc 0.83
(Sand 3%		R $3 \cdot 10^{-5} n_{y(14)}$

3.2 Slope Shape and Test Method

Fig.2 shows the shape of the model composed of circular and logarithmic spiral curves that cross with radial direction by the angle of 90° and 45° respectively.

In Test A, the consolidated soil block was shaped into the slope in the container, whereas in Test B it was first cut into λ-line in Fig.2 and was consolidated by self-weight under 80g for 45hrs, water level being kept above λ-line, and then shaped into the slope. After the markers were embedded on one side of the model, the containers were hung to the centrifuge, and was begun to run. The acceleration was increased continuously at the rate of 15g/min. till the slope failure took place, while the photographs were taken at every 5-10g. The test specimen is considered to keep undrained condition during this procedure.

By this method of increasing acceleration continuously up to the point of failure, the model passes variable self-weight stresses and strains similar to the prototypes of variable sizes. As soil is not elastic material this specific stress history may affect the strains at each stage to some extent, but is considered not to have much influence for the present investigation.

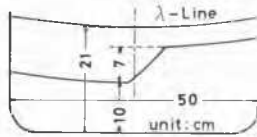


Fig. 2 Shape of the model

3.3 Method of Measurement of Deformation

Two methods were used to observe the process of deformation of the model. The point marker method is aimed to study the displacements and the strains in the slope quantitatively. The nail shaped point marker has a white cross of 0.2mm width on its head. About 200 of them are embedded on the slope section, forming a net with about 300 triangles of one side 2-3cm, that covers the slope section.

In the stripe marker method thin sticks of kneaded flour called "sohmen", which are hard in dry state but easily softened by moisture, are used. Slip lines and cracks are hard to catch by point marker method, but can be caught visually by stripe markers.

From the photographs taken during the test, six were selected at proper stages of deformation (Table II), and were projected to the real size. Then location of every point marker was read with the device capable to distinguish to 0.01mm.

Principal strains and maximum shear strain of each triangular element were calculated from the displacement of apexes and diagrammed using X-Y plotter. In each of Test A and B, the photograph at 30g was chosen out as the standard (stage 0) slope, because irregular settling of the model and markers is predominant and, also, is almost completed by this stage.

Table II Acceleration on each stage

Stage Test	0	1	2	3	4	5
A	30.0 g	80.9	97.4	102.4	110.0	124.6
B	30.0 g	90.2	105.0	120.0	140.9	149.9

4. TEST RESULT

4.1 Test on Slope of Uniform Strength (Test A)

Fig.3 shows the locus of point markers passing six stages from stage 0 to 5. The soil mass in the active zone slid rather straightly toward the bottom compressing the soil mass in the passive zone horizontal-

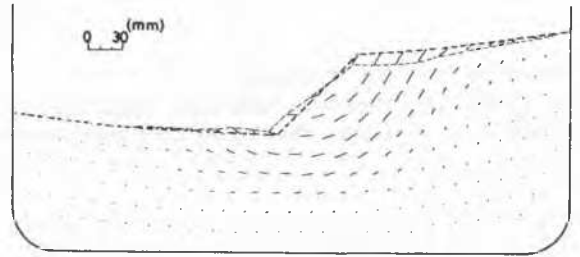


Fig. 3 Locus of the point markers
Stage 0-5, Test A : $H_p=2.1 - 8.7m$
(H_p : Height of prototype slope)

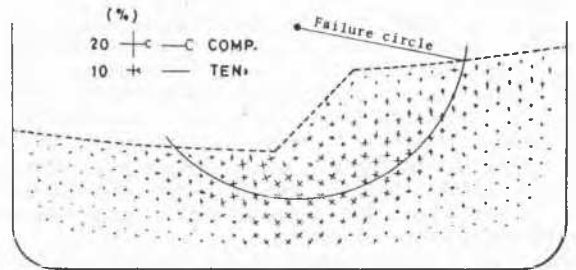


Fig. 4 Distribution of principal strains
on stage 4, Test A : $H_p=7.7m$

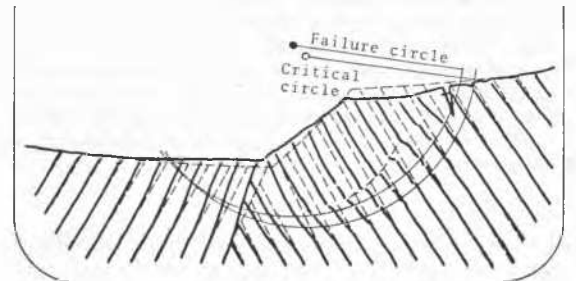


Fig. 5(1) Deformation by stripe markers
on stage 5, Test A : $H_p=8.7m$

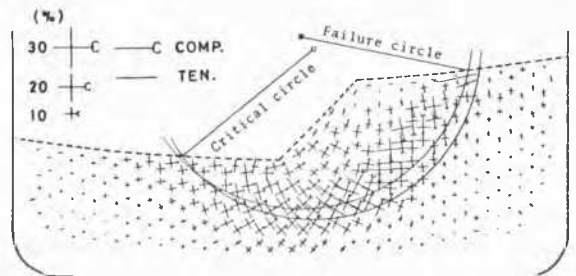


Fig. 5(2) Distribution of principal strains
on stage 5, Test A : $H_p=8.7m$

ly on earlier stages and somewhat upwards on later stages. The displacement is maximum at the top of slope and decreases toward the toe.

Fig.4 shows the distribution of principal strains on stage 4 (when the prototype slope height is $H_p=7\text{cm}$ $\times 110=7.7\text{m}$), most of which are combination of compression and tension of almost the same magnitude, which means that very little volume change was seen in every element. The distribution of strain along the potential failure circle is not uniform and the maximum value amounts to $\pm 5\%$ at the lower part of the active zone. A tension crack of 1.5cm depth was observed first on this stage.

Fig.5(1) and (2) show the deformation and distribution of principal strains on stage 5. The strains at the lower part of the active zone reached to $\pm 20\%$. Several short slip lines appeared in the active zone first on this stage, and the tension crack developed to 4cm depth. Throughout the test, no slip line was seen in passive zone, and the deformation as a whole clearly showed the process of progressive failure.

4.2 Test on Slope of Non-uniform Strength (Test B)

Fig.6(1) and (2) show the deformation and distribution of principal strains of Test B on stage 5. A toe failure accompanying a tension crack of 1.8cm depth took place. In the vicinity of the toe, the maximum shear strain reached 30-35%. This slope also underwent the process of progressive failure.

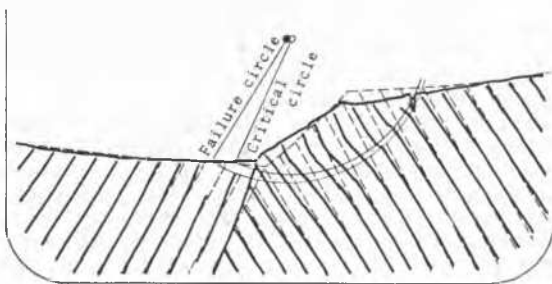


Fig. 6(1) Deformation by stripe markers on stage 5, Test B : $H_p=10.5\text{m}$

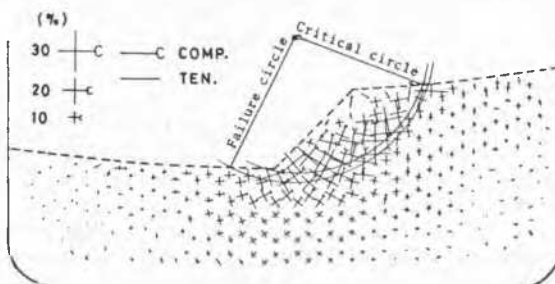


Fig. 6(2) Distribution of principal strains on stage 5, Test B : $H_p=10.5\text{m}$

5. STABILITY ANALYSIS OF THE SLOPES

5.1 Estimation of Strength by Cone Test

To measure the strength of the material in the same condition as the model slope under test, a small cone penetrometer was developed. The cone has a section area of 1cm^2 and an angle of 60° , and is driven by air pressure supplied through pneumatic slip ring on the

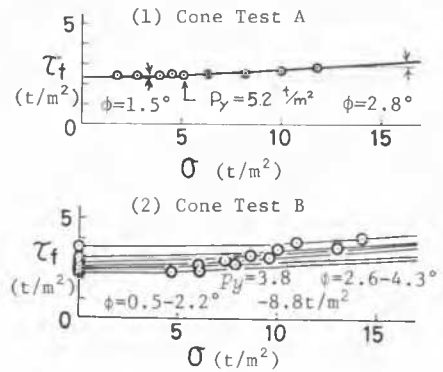


Fig. 7 σ - τ_f relationship by cone test

center shaft of the centrifuge.

Fig.7 shows the results of cone test A and B carried out for the model grounds prepared in the same way as Test A and B respectively. From cone test A carried out under $80g$ and $130g$, a unique σ - τ_f relationship, expressed in terms of total stress, was obtained showing consolidation yield stress*1 of $p_y=5.2\text{t/m}^2$. From cone test B carried out under $1g$, $100g$ and $130g$, a σ - τ_f relationship was obtained for every 2.5cm depth and six different lines were obtained as shown in Fig. 7(2). p_y value on each line is equal to the effective overburden pressure after the self-weight consolidation is completed under $80g$ at each depth.

5.2 Safety Factors of the Slopes

Safety factors F_s of the model slopes were calculated on every stage by the generalized "total stress analysis" method (Mikasa, 1963) using the well known equation (1)*2.

$$F_s = \frac{1}{\sum W \sin \alpha} \cdot \sum [c \cdot l + (W \cdot \cos \alpha - u_w \cdot l) \tan \phi] \quad (1)$$

In this method the strength parameters c and ϕ are determined in terms of total stress from the shear test under the same drainage condition as in the problem to be analyzed. In Test A and B, they were determined from Fig.7. The pore pressure u_w in the equation, accordingly, is not the one at failure, but is the one determined by ground water conditions. In Test A, the water level was assumed to be at the level where the effective overburden pressure p is equal to the consolidation yield stress p_y , because a soil just consolidated under p_y tends to consolidate or swell when it is subjected to the stress $p > p_y$ or $p < p_y$ respectively. In Test B, it was assumed to be at the level of the top of the slope on stages over $80g$, as the self-weight consolidation and swelling under $80g$ are considered to have almost completed already.

*1 "Consolidation yield stress p_y " was named by the present senior author for the "pre-consolidation stress p_c " to make clear the physical meaning of the property.

*2 Bishop's equation was also used in place of Eq.(1) in the analysis of the test with the same c, ϕ and u_w value and yielded F_s value that is different from Eq.(1) only by 0.01 (as ϕ value is rather small). Thus the results by Eq.(1) alone are presented in this paper.

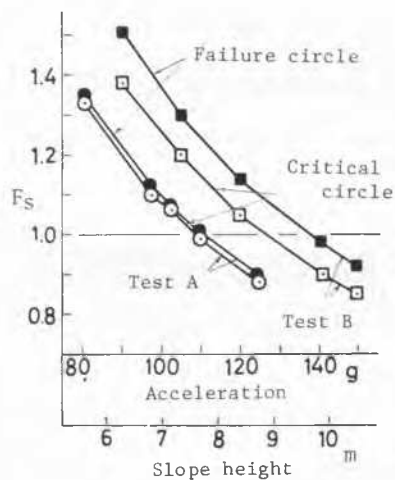


Fig. 8 Safety factors by Eq.(1)

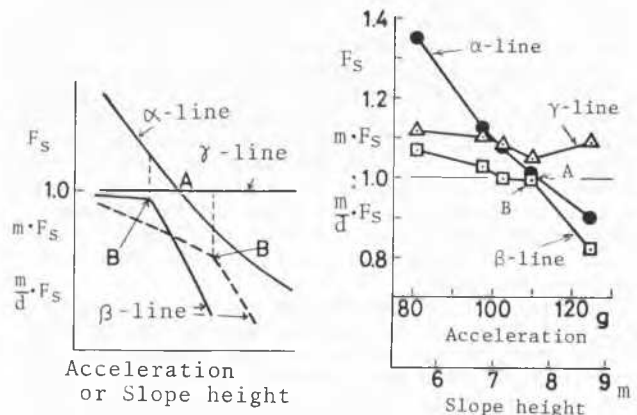
Fig.8 shows the results of calculation at five stages in Test A and B. The critical circle, which has the minimum safety factor among 250 trials, and the failure circle drawn on the figures of stage 5 so as to pass the lower end of the tension crack, are shown in Fig.5 and 6. In both tests two circles are located very near. And F_s value came down below 1.0 on stage 4, when cracks were first found. These results may be said to demonstrate the validity of the method of analysis and the strength parameters used here in a practical sense.

5.3 On the Effect of Strength Mobilization and Slope Deformation for the Slope Stability

As shear strains were found not to be uniform along the failure circle on any stage of the test, the degree of mobilization of shear strength is not uniform either. The ratio of mean mobilized shear strength to the peak strength is named here as 'mobilization factor m ', which increases up to the failure point and decreases thereafter, and always takes the value not larger than 1.0. It should also be noted that along the progress of stages the sliding moment changes because of the slope deformation. The ratio of sliding moment evaluated from the deformed slope shape to that obtained from the original one is named as 'deformation factor d ', which decreases from 1.0 with the progress of deformation of slope.

The sliding force taking into account the slope deformation and the mobilized resisting force will be well balanced except in the case of an abrupt failure, and the value of $m/d \cdot F_s$ will be 1.0 throughout the test, which is shown as γ -line in Fig.9(1). β -line represents the locus of $m \cdot F_s$ in which the degree of strength mobilization only is taken into consideration. The point B on β -line, at which the mobilization factor takes maximum value of $m_{max} \cdot F_s$ (< 1.0), may be defined as the failure point of the slope. And the safety factor that should be used in design works is not F_s but $m_{max} \cdot F_s$ ($< F_s$) theoretically. This failure point B may be located to the left or right of point A, at which $F_s = 1.0$, depending upon the stress-strain characteristics of the soil and the type of slope.

Fig.9(2) shows the three lines of F_s , $m \cdot F_s$ and $m/d \cdot F_s$ calculated for the failure circle of Test A. α -line that shows safety factors F_s is the same as in Fig.8. Mobilization factor m on each stage was esti-



(1) Schematic diagram

(2) Results of Test A

Fig. 9 Value of F_s , $m \cdot F_s$ and $m/d \cdot F_s$

mated from the observed distribution of shear strain along the failure circle and the stress-strain relationship obtained from a consolidated constant-volume direct shear test using the improved type direct shear tester (Mikasa, 1965), as the specimen depth of which is almost the same size as the distance between adjacent point markers. Deformation factor d was evaluated from the observed slope shape on each stage.

The mutual relationship between the three lines is similar to the schematical diagram in Fig.9(1), and in this case the failure point B on β -line locates very near to point A, when $F_s = 1.0$.

$m/d \cdot F_s$ on γ -line did not take the value of 1.0 as was expected, but of 1.05 - 1.1 throughout the test. This may be due to the inaccuracy of the assumptions in the shape of the failure surface, strength parameters, ground water level and the degree of strength mobilization, for which further investigations are needed.

ACKNOWLEDGEMENT

The authors wish to thank to Mr. N. Takada for his helpful and instructive suggestions. The assistance of Mr. J. Adachi and Mr. R. Hasegawa in the experimental works is also acknowledged.

REFERENCE

- Mikasa, M. (1963), On the Strength of Clay -- Critical Review on the Effective Stress Analysis --, "Tsuti to Kiso" (Journal of the Japanese Society of SMFE), Vol.11, No.2, p.31 (in Japanese)
- Mikasa, M. (1965), On the Apparatus and Testing Method of Tri-axial Test and Direct Shear Test, The 10th Symposium of Japanese Society of SMFE, p.117 (in Japanese)
- Mikasa, M. and Takada, N. (1973), Significance of Centrifugal Model Test in Soil Mechanics, Proc. The 8th Int. Conf. SMFE, Vol.1, p.273
- Mikasa, M. and Mochizuki, M. (1975), Centrifugal Model Test of Sensitive Clay Slopes, The 4th South-East Asian Conf. SMFE, p.5-19